Fast soliton-like charge pulses in insulating polymers

L. A. Dissado,[1] G. C. Montanari,[2] and D. Fabiani[2,a)]
[1]*Department of Engineering, University of Leicester, Leicester LE1 7RH, U.K.*
[2]*LIMAT Department of Electrical Engineering, University of Bologna, Bologna, BO 40136 Italy*

(Received 29 July 2010; accepted 14 January 2011; published online 18 March 2011)

A previously unknown mode of conduction is identified in insulating polymers at moderate fields (40–50 MV/m). This takes the form of coherent charged pulses with a mobility ($\sim 10^{-10}$ $m^2V^{-1}s^{-1}$) several orders of magnitude larger than that traditionally associated with independent charge carriers ($\sim 10^{-14}$ $m^2V^{-1}s^{-1}$). It is shown that this phenomenon is consistent with a mechanism in which a charged compression boundary is formed electro-mechanically during injection and thereafter travels as a coherent solitary wave (soliton) through the polymer. © *2011 American Institute of Physics*. [doi:10.1063/1.3554694]

I. INTRODUCTION

Insulating polymers are commonly regarded as wide bandgap semiconductors with a large number of local states within the bandgap.[1–3] The electrode contacts are nonohmic with an energy barrier for charge injection. At low fields (up to E ~10 MV/m at 20 °C in polyethylene) impurities supply a low concentration of carriers ($\sim 10^{15}$ –10^{16} m^{-3}) as do the contact charge regions at the electrode interface. At higher fields charge injection from the electrodes is expected to lead to space charge and space charge limited currents.[4–7] Localized intra-band states that act as charge traps are assumed to govern the macroscopic carrier mobility, with the dwell time in the traps determining the carrier mobility.[3] For the last 20 years it has been possible to quantitatively measure the space charge concentration within an insulator by means of pressure wave propagation (PWP) and pulsed electroacoustic (PEA) techniques[8–12] as a function of the time of application of the potential difference (or subsequent to its removal) and hence to determine directly the charge dynamics, thereby allowing a direct comparison of theoretical expectations with experimental data. Recently the time resolution of the PEA technique has been improved such that a complete profile of the space charge density can be obtained every 25 ms.[11,13,14] Application of the technique to miniature cables possessing a thickness of 1.5 mm of Cross-Linked-Polyethylene (XLPE) (Fig. 1) have revealed that at moderate fields (30 MV/m to 50 MV/m) the injection of charge instead of being continuous,[15] takes the form of small pulses (containing approximately $3–6 \times 10^9$ electronic charges) that transit the insulation at speeds several orders of magnitude greater than those estimated from steady state currents in XLPE. Both positive and negative pulses are observed that not only retain their shape and amplitude during transit, but which have also been noted to pass one another in the same plane without alteration. Such behavior is not consistent with the incoherent motion transferring carriers from trap to trap as the insulation material is transited. This is a new conduction phenomenon that challenges traditional approaches to charge transport in insulating polymers. We shall show that the pulse generation and transit is consistent with a model that treats a pulse as a quantum of charge able to activate boundary compression (through electric field modification) and consequently that pulse charge motion can occur thanks to the electro-mechanical effects of the electric field alteration in compressible materials such as many insulating polymers.

II. MATERIALS AND EXPERIMENTAL METHODS

The measurements were carried out on 1.5 m lengths of commercially produced XLPE insulated miniature cables (Fig. 1) whose insulation thickness is 1.5 mm. The XLPE layer is surrounded by an inner and outer layer of polyethylene loaded with carbon particles that provides a weakly conducting connection to the inner metallic conductor and a metallic outer conductor. These layers are commonly termed semicon (semiconductive) by industrialists, but this implies no relationship to solid state semiconductor materials. The as-received cable sections are kept at 80 °C for 5 days in order to expel volatile by-products produced during the *in situ* cross-linking of the polyethylene and also any remnant solvent from the carbon-loaded polyethylene layers, and then placed in an electrically-isolated controlled-temperature environment. A DC potential difference was applied between the inner metallic conductor and an aluminum plate in contact with the outer carbon-loaded polyethylene layer that acts as a ground electrode and measurements of the space charge distribution were made over a range of times for average fields of 40 and 50 MV/m at temperatures of 308 K, 323 K, and 343 K. This was carried out by means of the Pulse-Electro-Acoustic (PEA) technique,[16–19] the basis of which is that a probe voltage pulse (in this case of 1500 V and 40 ns duration) is superimposed on the much higher continuously applied DC voltage, which causes a change in the electro-mechanical stress where space charge exists and hence generates an acoustic compression or rarefaction pulse that is detected by a piezo-electric detector located under the ground electrode. The pressure wave profile has the same shape as that of the space charge, and its amplitude is proportional to the space charge density. Its form (compression or rarefaction) gives the charge polarity, and the delay between its detection and the voltage pulse application gives the space

a)Electronic mail: davide.fabiani@unibo.it.

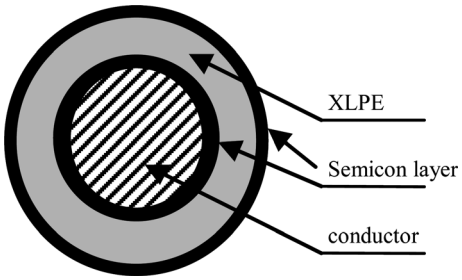

FIG. 1. Sketch of tested minicable. Conductor diameter = 2.8 mm; Inner semicon thickness = 0.7 mm; dielectric (XLPE) thickness = 1.5 mm. Outer semicon = 0.15 mm.

charge location, since the acoustic pulse travels at the known speed of sound in the material. A discussion of the theory behind this and similar techniques have been given by Holè *et al.*[20] This weak voltage signal is then amplified by two wide-band amplifiers, and sent to an ultra-fast-data-acquisition system. The probe-voltage pulses have a 2 kHz repetition frequency and each space charge profile is a digital average of 100 piezo-electric signals performed in order to have a good signal to noise ratio. This allows a complete radial profile of the space charge to be acquired every 25 ms, with an amplitude resolution[21] of 0.03 Cm^{-3}. The piezo-electric response is an average across the area of the detector hence the spatial resolution is limited to the radial direction and is determined by the width of the probe voltage pulse, the detection system bandwidth, and signal processing,[22] which in the system under discussion would cause a plane of charge to be broadened to a Gaussian peak of roughly 60 microns width.

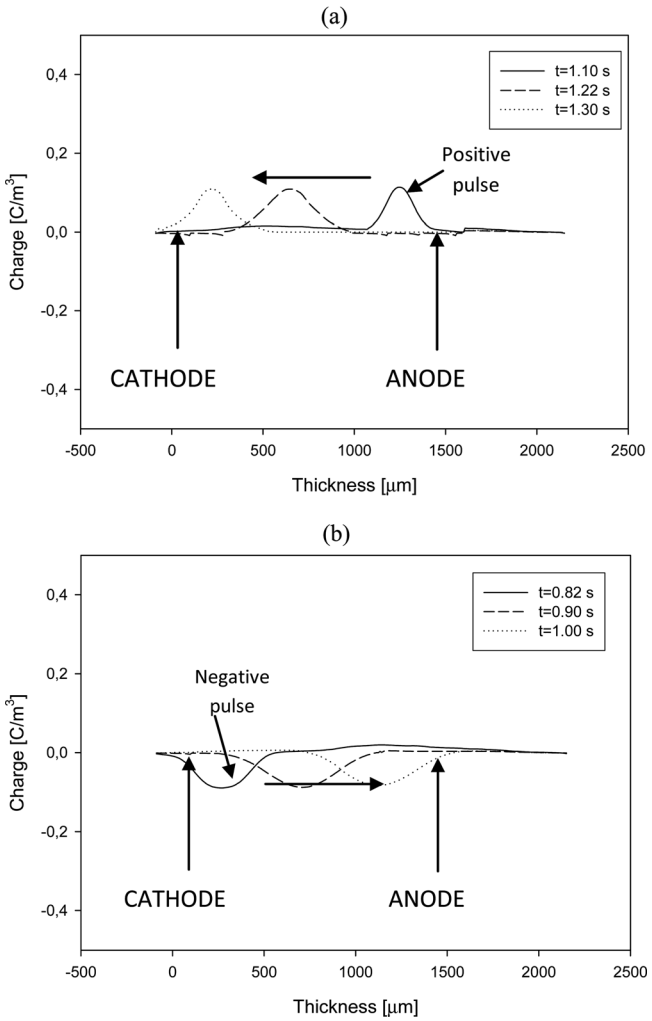

FIG. 2. Time-dependent space charge profiles. (a) Positive pulses crossing the insulation, (b) negative charge pulses crossing the insulation, with the arrow indicating pulse direction. The pulses are evidenced by subtracting the profiles of the first space charge data acquisitions from the charge profiles at time t, after de-noising by means of Wavelet Transform (Ref. 13). The time relevant to each profile acquired is reported in the legend. The space charge profiles are measured at E = 40 kV/mm, T = 45 °C.

TABLE I. Pulse characteristics at E = 40MV/m T=308 K.

Pulse polarity	Charge/Area [Cm^{-2}]	Charge [C]	Repetition Rate [s^{-1}]
Positive	2.0×10^{-5}	1.0×10^{-9}	3.3
Negative	1.0×10^{-5}	5.0×10^{-10}	2.5

III. RESULTS

The space charge measurements showed the existence of a persistent series of charge pulses of both polarity that crossed the insulation layer in a fraction of a second, examples of which are shown in Fig. 2. Their repetition rate was found to be dependent only upon temperature and electric field, as will be shown in the following, see Tables I–IV. Measurements made every 25 ms for the first minute of voltage application allowed between 100 and 200 such pulses of each polarity to be observed. It was noted that: (a) the shape of each pulse was retained during its transit of the insulating layer, (b) the amplitude of the pulses exhibited a polarity dependence though all pulses of the same polarity had the same amplitude and showed little dependence upon field and temperature,[23] (c) the speed of transit was independent of radial position (within our time resolution) but depended upon temperature and field and polarity, (d) the pulse repetition rate was polarity dependent at the same temperature and field, resulting in situations where both a positive and negative pulse moving in opposite directions were present in the XLPE layer at the same time, Fig. 3. In this case the pulses recovered their amplitude once they had passed through the same plane (where the measured space charge density was the net value of that of the two pulses). The constant speed (v) of the pulses allow us to determine the mobility (μ) of the pulse in the average field E_{av} via

$$\mu = v/E_{av}. \tag{1}$$

TABLE II. Pulse mobility (in $m^2V^{-1}s^{-1}$) in mini-cables.

Pulse Polarity	Field [MV/m]	T = 308 K	T = 318 K	T = 333 K
Positive	40	7.19×10^{-11}	9.60×10^{-11}	1.90×10^{-10}
	50	1.24×10^{-10}	1.64×10^{-10}	2.98×10^{-10}
Negative	40	9.58×10^{-11}	1.44×10^{-10}	5.75×10^{-10}
	50	1.79×10^{-10}	2.68×10^{-10}	8.51×10^{-10}

TABLE III. Number of pulses per second in mini-cables.

Pulse Polarity	Field [MV/m]	T = 308 K	T = 318 K	T = 333 K
Positive	10	—	—	1
	15	—	1	2
	25	1	3	3.5
Negative	10	2	2.5	3
	15	2	3	3
	25	2	3	3.5

A summary of the data (pulse charge/area and mobility) is given in Tables I and II. The pulse repetition rate as a function of field and temperature is reported in Table III.

Charge pulses have been observed previously in similar materials at $E \geq 80$ MV/m[18,24–27] however in those cases the pulses often show variations of amplitude both during transit and over a sequence of pulses, and more importantly a mobility ($\mu = 10^{-16} - 10^{-15}$ $m^2V^{-1}s^{-1}$), and activation energy (1–1.2 eV)[13,27] close to that of the carriers in steady state currents. Explanations for these pulses have been proffered in terms of a negative differential resistance,[28] imbalance between injection/extraction and transport[29] or a dc-conductivity discontinuity.[30] However the current observations differ in the following important points: (a) the charge pulse always initiates from the electrode interface and contains a polarity specific quantity of carriers, and (b) the mobility of the carriers as a coherent group is many orders of magnitude higher than the carrier mobility determined from steady state currents in Polyethylene ($\mu = 10^{-15} - 10^{-14}$ $m^2V^{-1}s^{-1}$).[31]

IV. MODEL

An explanation for the charge pulses observed requires both the generation of charge pulses by an injection current that reduces rapidly to a negligible value as the injection proceeds and the movement of a charge pulse into the body of the polymer without allowing further injection to take place. These requirements can be fulfilled by realizing that the polymers under investigation will be compressed electromechanically by an electric field, which will be largest locally at the electrode-polymer interface, e.g., due to the presence of an electrical double layer there.[32] This will facilitate tunneling of packets of electrons between surface states of the electrode, in this case conducting carbon particles, and

TABLE IV. Number of pulses per second observed on cable with a different carbon-loaded electrode but the same XLPE insulating material.

Pulse Polarity	Field [MV/m]	T = 308 K	T = 318 K	T = 333 K
Positive	10	0.25	0.25	—
	15	0.5	0.25	1
	25	0.5	0.5	3
Negative	10	—	—	—
	15	—	0.25	—
	25	0.5	0.5	4

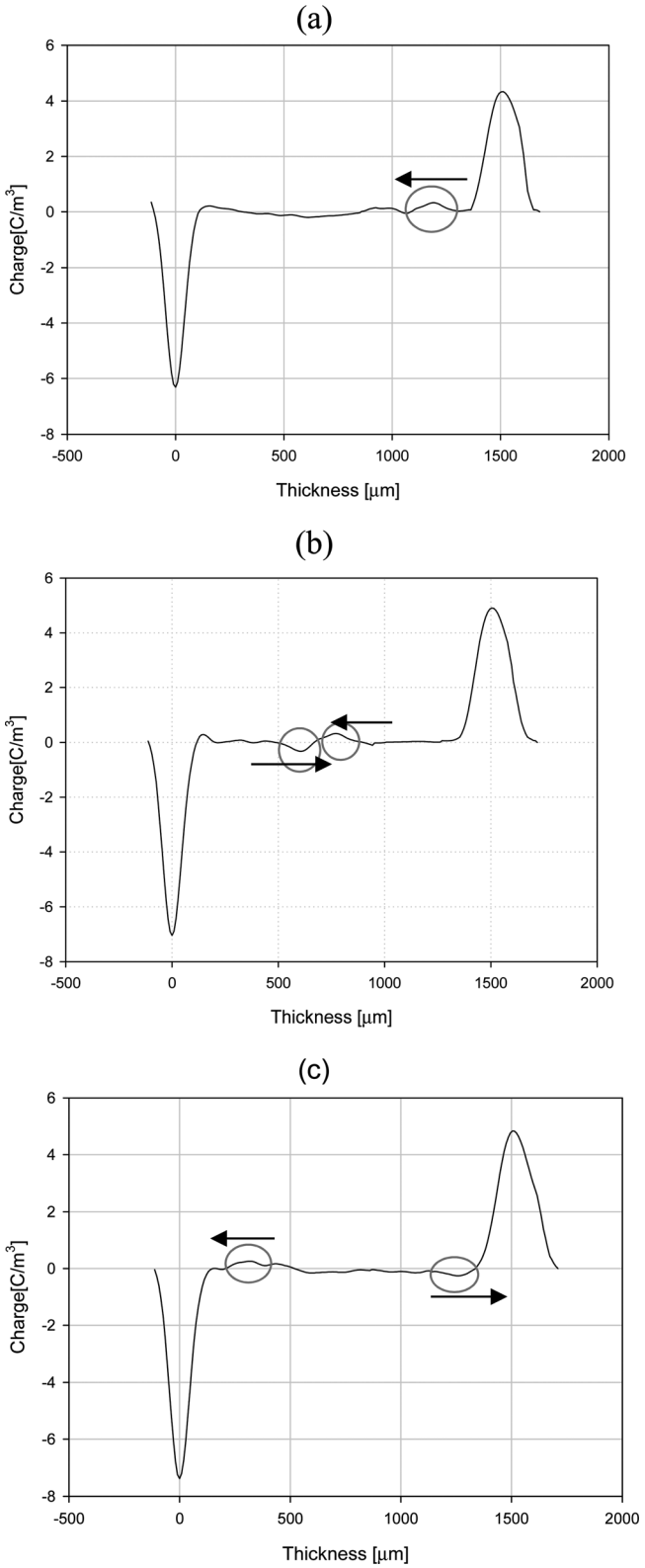

FIG. 3. Time sequence of space charge profiles detected in XLPE minicables every 50 ms. E = 40 kV/mm, T = 70 °C. The positive and negative charge pulses are evidenced by gray circles. The arrows indicate the pulse movement.

sites in the polymer, at fields and temperatures where field-assisted thermal promotion over the injection barrier (i.e., Schottky injection; see Taylor *et al.*[33] for a review of this process in polymers) would be very weak. As the tunneling

injection proceeds the reduction in electrode-interface local field will reduce the compression allowing the charge to move with the polymer displacement, and hence increasing the tunneling distance and reducing the injection current. At the same time the field in front of the injected charge will build-up increasing the compression at the boundary between the charge and the remainder of the polymer. This allows the charges to transfer coherently to sites in the newly compressed region faster than they can move by independent trap to trap hopping. The fast charge transport will then be maintained as long as the charge and the compression boundary move together as a single entity, i.e., they move as a charged solitary wave, a soliton.[34,35]

A. Pulsive injection

The injected pulse is assumed to be a plane of charge (Q_p) giving a reduction in field at the injecting electrode of

$$\delta E = Q_p/2A\varepsilon. \tag{2}$$

A is the area of the injecting electrode, and ε is the polymer dielectric permittivity (2.03×10^{-11} Fm^{-1} for the XLPE under test). Since electro-mechanical stress is proportional to E^2 the field reduction due to the pulse gives a reduction in radial compression of

$$\delta = hE\delta E, \tag{3}$$

where h is a material related coefficient.

The data in Lewis *et al.*[32] allows $h = 1.56 \times 10^{-23}$ $V^{-2}m^3$ to be estimated for polyethylene, giving $\delta_p \sim 0.3$ nm for our experimental data (positive pulses, $\delta E = 4.9 \times 10^5$ Vm^{-1}) and $\delta_n \sim 0.15$ nm (negative pulses, $\delta E = 2.45 \times 10^5$ Vm^{-1}), at $E = 40$ MV/m.

Positive pulse injection requires the tunneling of an electron from the C-C bonds of the polymer chain into the surface states of the electrode. As the field due to the injected charge builds up the polymer chains displace according to Eq. (3) and carry the injected charge with them. The process is modeled through a tunneling injection current density, $J_{inj}(t)$, whose value depends upon the position of the displacing chain at time t after injection is initiated.

$$J_{inj}(t) = J_o \exp[-2\alpha\delta(t)]. \tag{4}$$

J_o is the initial injection current, whose value depends upon the tunneling distance at initial compression and any possible thermal activation necessary to equalize the electron energy with that of the electron accepting states, α is the tunneling coefficient. The increase in tunneling distance $\delta(t)$ at a time t after the start of charge injection, is calculated from Eq. (3) using the field reduction $\delta E(t)$ due to the previously injected charge (Eq. (2)), with Q_p/A obtained by integrating the injection current density up to t. In Lewis *et al.*[32] the displacement in polyethylene due to an applied sinusoidal δE is independent of frequency in the range 10–10^3 Hz, so we have assumed that the mechanical displacement of the polymer chains is fast enough to allow it to be synchronous with the buildup of injected charge. The tunneling coefficient α is calculated from the WKB approximation for a square barrier of magnitude Δ

$$2\alpha = (4\pi/h)(2m)^{1/2}\Delta^{1/2}, \tag{5}$$

using a value of $\Delta = 1.7$ eV for positive charge injection taken from typical experimental values for interfaces between XLPE and carbon-loaded polymer.[36] The same source gives the barrier height for negative charge (electron) injection as 1.65 eV. Because of the unknown factors involved in calculating J_o, we have used it as a fitting parameter with a value chosen to fit the maximum injection current measured and such that the observed pulse charge is injected before the current becomes negligible. This makes the model of injection a demonstration of feasibility rather than an exact replication of experimental data.

Figures 4(a) and 4(b) show a numerical simulation of the positive pulse injection current density and charge density, respectively, as a function of time at 0.3 nm from the electrode. The formation of a positive pulse during injection is displayed in the 3D-plot of Fig. 4(c). Figures 4(a) and 4(b) evidence that the injection is almost complete ($J_{inj}(t)/J_o \sim 0.015$) within 10 ms at which time the plane of charge has moved a distance of about 0.3 nm into the polymer, as illustrated in Fig. 4c, with the penetration slowing down as the injection current reduces.

The calculated pulse generation time is only a small part (i.e., ~2.5%) of the transit time of the pulse transit across the XLPE layer and is much less than the time between positive pulse repetitions (~300 ms at $E = 40$ MV/m $T = 343$ K) and is consistent with our observations.

The injection of negative pulses can be described in a similar way, i.e., through electron tunneling to trap states on the polymer chain. Here, however, a chain displacement of $\delta R = 0.15$ nm (appropriate to the negative pulse charge) gives a reduction of injection current to only ~0.14 J_o, a value that seems too high. Since polyethylene has a negative electron affinity (i.e., the conduction level lies above the vacuum state)[37] the more likely locations for the injected electrons are free volume regions (1–10 nm in size) where potential lattice sites for the carbon atoms of the polymer chain are unoccupied by polymer atoms[38] due to steric hindrances between the polymer chains, which results in a lower macroscopic density than that which would obtain for the polymer crystal. In this case chain displacements corresponding to the local shear produced by the initial field-generated compression would open up free volume regions to abut the electrode, and tunneling would take place to energy states within this small box.[28] As the injected charge causes the chain displacement to relax, the receiving sites for the tunneling electrons will move further into the polymer than the chain displacement, and the barrier for injection would increase due to the intervening polymer. Under these conditions Δ in Eq. (5) would increase beyond our assumed value and the tunneling distance at the end of the pulse injection could be around a nanometer rather than the 0.15 nm of the chain displacement. Both these factors reduce the tunneling current to a negligible value when the chain displacement has removed easy access to the free volume box.

B. Pulse transport

While the generation of a charge pulse relies upon the field reduction between itself and the injecting electrode to

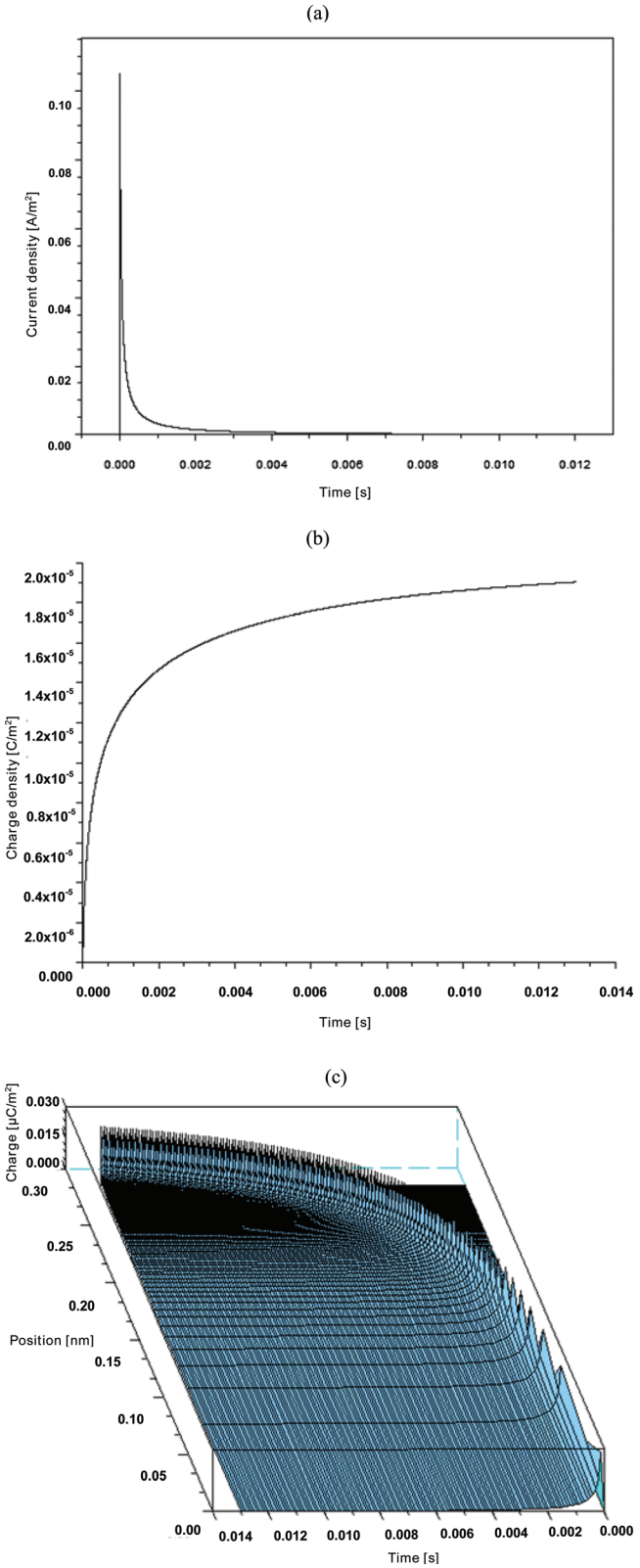

FIG. 4. (Color online) Simulation of positive pulse injection. (a) Positive pulse injection current density as a function of time; (b) positive pulse injection charge density as a function of time at 0.3 nm from the electrode (c) 3D plot showing the formation of a positive pulse during injection.

prevent further injection its transport requires the compression at its boundary due to the consequent increase in electro-mechanical stress. The compression is composed of specific forms of local polymer chain displacement and the time taken for the chain section to relax to its displaced position is dependent upon the form (mode) of the relaxation via a mode-specific activation energy, which takes into account the number of atoms involved and the polymer hindrances that need to be surmounted. Polyethylene is a semicrystalline polymer[39] with crystal lamella separated by amorphous low density regions of tangled polymer chains that also tie the lamella together. Two modes of chain displacement are responsive to a mechanical stress and both relate to relaxations that occur in the amorphous region.[39] In the β-mode segments of polymer chain flex as a group with a reported activation energy in the range 0.5–0.75 eV.[40] The γ-mode corresponds to the 180° rotation of at most a few C-C bonds about a chain axis. This feature can move along a chain section as a chain kink or in the form of a crank-shaft motion. The activation energy for this relaxation mode is reported to be ~0.25 eV.[40]

The segmental bending of the β-mode relaxation is the displacement most likely to open up free volume to access by the injected electrons. For example Fig. 5(a) shows how this may be achieved by small shear displacements of a flexible section of polyethylene chain that are consistent with a compression of 0.15 nm (appropriate to the negative pulse). The time taken for a β-mode displacement to create an opening into neighboring free volume will be orders of magnitude longer than that required for the motion of the electron to carry it into the free volume under the action of the electric field ($\sim 10^{-14}$ s). The speed of advance of the negative pulse will therefore be governed by the relaxation rate of the β-mode $((2kT/h)\exp(-\Delta U_\beta/kT))$, where h is Planck's constant and ΔU_β is the field-independent activation energy for the β-mode. The coupling of the electron and the β-displacement as a coherent entity (the pulse) means that the energy of the electron in the electric field must be taken into account in determining the rate of advance, as also must the possibility of the reverse electron flow, i.e., the energy of the electron in the field reduces the energy required for a forwards movement and increase it for a reverse movement. This leads to an additional factor of $(\exp(eE_{av}R_s/2kT) - \exp(-eE_{av}R_s/2kT))$ in the net speed of electron advance, with the distance advanced being R_s, i.e., the mean size of the free volume in the field-direction. The pulse mobility then takes a form similar to that proposed for the trap-to-trap hopping of electrons in an electric field.[1,4,31]

$$\mu(E_{av},T) = \frac{rate.R_s}{E_{av}} = \frac{2kTR_s}{hE_{av}}\exp\left(-\frac{\Delta U_\beta}{kT}\right)\sin h\left(\frac{eE_{av}R_s}{2kT}\right). \tag{6}$$

Since R_s will be the size of a free volume region, i.e., some nanometres, rather than the distance displaced by the polymer chains to open up access, $eE_{av}R_s/2kT > 1$ at the fields considered and hence

$$\mu(E_{av},T) = \frac{kTR_s}{hE_{av}}\exp\left(-\frac{\Delta U_\beta}{kT}\right)\exp\left(\frac{eE_{av}R_s}{2kT}\right) = \frac{kTR_s}{hE_{av}}\exp\left(-\frac{\Delta U_\beta - eE_{av}R_s/2}{kT}\right). \tag{7}$$

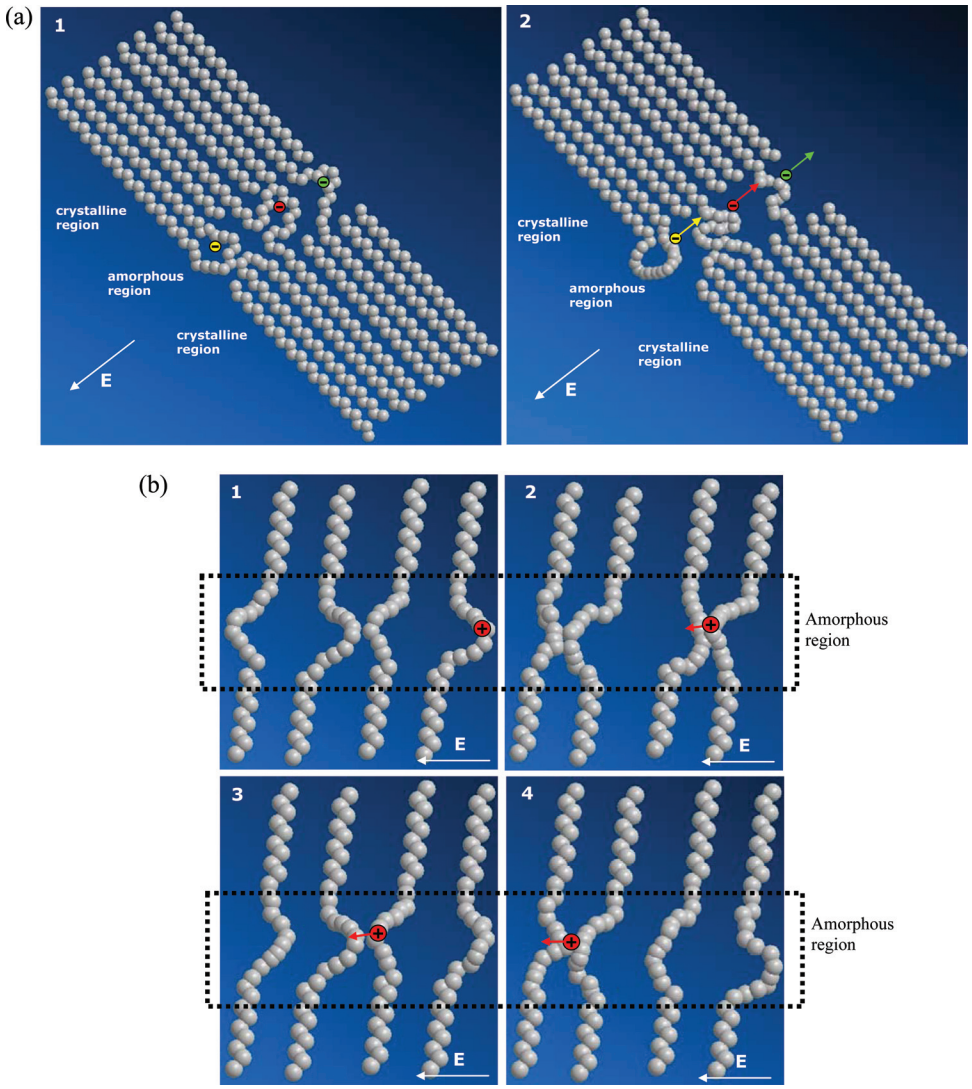

FIG. 5. (Color online) Charge pulse movement scheme. (a) Negative charge movement via polymer β-mode displacement in the amorphous region. The electric field direction is indicated by an arrow. (1) Three negative charges (yellow, red and green) moving in the free volume are blocked by polymer chain bends in the amorphous region. (2) Chain β-motion causes the walls of the free volume in the amorphous region to open allowing charges to move under the action of the electric field to the walls of the next free volume region. (b) Positive charge packet movement by means of crank-shaft displacement of the polymer chains in the amorphous region. (1) Positive charge (in red) is located inside the first polymer chain in the amorphous region. (2–4) Kink motion allows the chain with the charge to approach close enough to a neighboring chain to allow the charge to transfer from one chain to the other by electron tunneling.

The apparent activation energy, $\Delta U_\beta - eE_{av}R_s/2$, in Eq. (7) is dependent upon E_{av}. This can be seen in the experimental data, see Fig. 6 where the lines show the fit to Eq. (7) with $R_s = 5$ nm and $\Delta U_\beta = 0.52$ eV, which are consistent with an advance of the negative pulse by the opening of free volume of average length 5 nm by a β-mode displacement.

The positive pulse can only advance by the reverse tunneling of electrons from a receiving polymer chain to the chain containing the positive charge.[28] This means that the enabling polymer displacement involved must bring C-C bonds on neighboring chains close together. The most likely candidate is the γ-mode, whose 180° rotation would move a few C-C bonds by about the 0.3 nm noted to be appropriate to the positive pulse charge transport. A schematic representation of the process is shown in Fig. 5b, where the tunneling occurs over a short distance of the order of the atomic radius of the carbon atoms ($R_t \sim 0.05$nm) and the positive hole in the valence bond is carried a distance $R_s \sim 0.3$ nm (at 40 MV/m) by the relaxing polymer. The positive pulse mobility therefore will be dependent upon the rate of relaxation of the γ-mode displacement. However in this case the tunneling probability ($\exp(-2\alpha R_t)$) between the two chains will also be a factor, though it should be noted that the activation energy barrier Δ and effective mass m may have different values to those obtaining during injection. Since $eE_{av}R_s/2kT < 1$, $\sinh(eE_{av}R_s/2kT) \approx eE_{av}R_s/2kT$ and the mobility becomes.

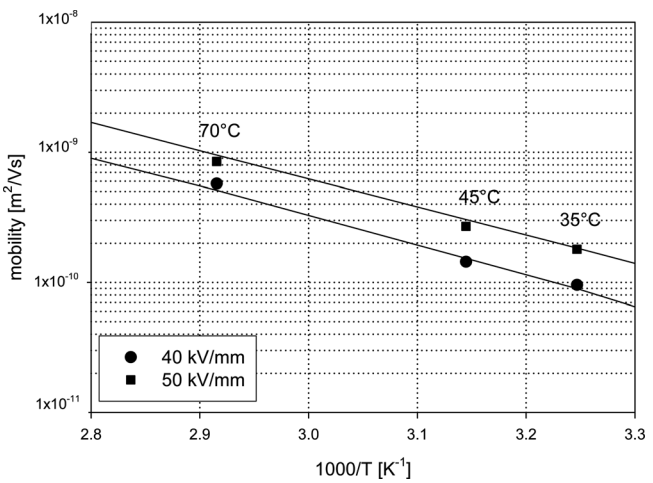

FIG. 6. Arrhenius plot of negative pulse mobility. The lines show the fit to Eq. (7).

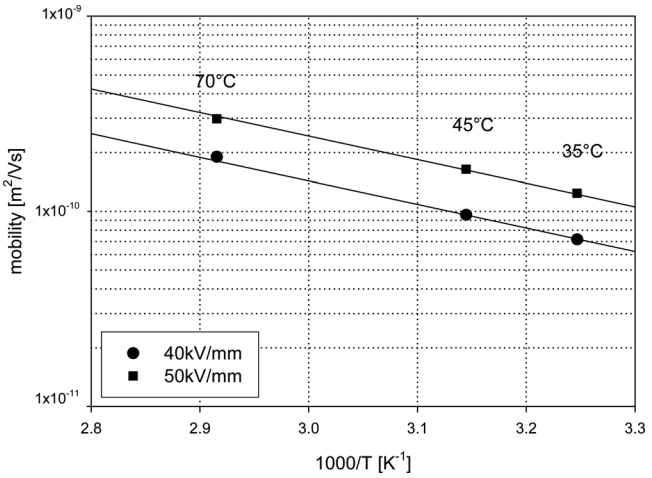

FIG. 7. Arrhenius plot of positive pulse mobility. The lines represent the fit to Eq. (8)

$$\mu(T) = \frac{eR_s^2}{h}\exp\left(-\frac{\Delta U_\gamma}{kT}\right)\exp(-2\alpha R_t). \tag{8}$$

Equation (8) predicts an activation energy that is independent of field as is found in the experimental data, Fig. 7, where the value obtained $\Delta U_\gamma = 0.24$ eV is consistent with the activation energy of the γ-mode relaxation displacement.[40] The value of R_s is that of the compression produced by the pulse charge in the applied field and is slightly field dependent (Eq. (3)). Use of the values $R_s = 0.32$ nm, $E = 40$ MV/m, and $R_s = 0.42$ nm, $E = 50$MV/m obtained from Eq. (3), allows Eq. (8) to be fitted to the experimental data with a common value of tunneling factor. The value obtained, $\exp(-2\alpha R_t) = 2.45 \times 10^{-2}$, is reasonable and indicates the necessity of local displacements in order to bring chains close enough to enable the tunneling transfer.

V. DISCUSSION

The existence of the charge pulses observed requires first injection in the form of discrete pulses of charge rather than a continuous current monotonically decaying to its steady state value. A mechanism for the formation of injected charge pulses based on a negative differential resistance would lead to a repetition of the pulse every time a pulse exited the system at the counter electrode allowing the initial field conditions to be recreated at the injecting electrode, such as can be observed for the slowly moving charge pulses generated at fields in excess of 80 MV/m.[25,26] This is not the case here. The mechanism that we have proposed generates an amount of charge locally in the pulse plane sufficient to reduce the current for tunnel injection to a negligible value as the charged plane moves into the polymer, and to maintain its further penetration as a transporting entity. As noted this amount (i.e., the charge pulse) will depend upon the change in electro-mechanical compression that it produces, and this will be only weakly dependent upon temperature and the fields used (40 and 50 MV/m). Since the total electro-mechanical compression is field-dependent[32] however, it may become too small to allow tunneling injection to be effective at lower fields, i.e., J_o becomes smaller than incoherent thermal promotion over the injection barrier. Table III indicates an onset field of ~10 MV/m for positive pulse injection, at 60 °C for XLPE. In our model the charge is injected from surface states of the electrode-polymer interface, and thus the repetition rate will be governed by the time required to replenish these states. Measurements on a different mini-cable of the same geometry made from the same batch of XLPE, but with different carbon-loaded polymer electrodes, Table IV, show that the repetition rate is dependent upon the electrode material, and hence upon the electrode-polymer interface (since we would expect the same transit time for the same field and temperature in the polymer, pulse repetition cannot be associated with the arrival of pulses of opposite polarity to the injecting electrode). The data in Tables III and IV show that the repetition rate is both field and temperature dependent, which would be consistent with a number of interface processes. The lack of detailed knowledge of the interface[28,41–44] however, makes it impossible to make an analytical calculation of surface charge replenishment via transfer of charge to surface states, either from the electrode or by ionisation of impurity molecules located in the surface region.

The second central feature of the observed pulses is a transport mechanism in which the pulse moves at a high constant speed while retaining its form. One requirement for this to occur is that the charges of which the pulse is formed move coherently as a unit, i.e., spreading due to diffusion or the small field difference (~0.5 – 1 MV/m) between the front and rear of the pulse is not effective. The exceptionally high pulse mobility, which is several orders of magnitude higher than the mobility of charges that carry DC steady state current, and the low-medium range of the field magnitude where the observations are made, preclude an explanation based on a negative differential resistance.[28] This is re-enforced by a repetition rate that is not based on the transit time of the polymer. The explanation that we have proposed regards the pulse as a moving charged compression boundary, with the coherent advance of the charge being essential to the movement of the compression boundary and vice versa. Under these circumstances the pulse moves too fast to allow any independent transport of its individual charges with the speed of sound forming an upper bound to its velocity, which is not reached in these experiments. Such a moving coherent entity is by definition a solitary wave,[35,45,46] i.e., the pulse is a charged soliton.[34] However, the amount of charge in the pulse will be determined by the need for it to produce a field large enough to produce the compression that will allow its advance as a coherent entity, rather than the single electron soliton of Bylander *et al.*[34] Table V shows that pulse charge/area depends on the insulating polymer (INS1 or INS2). Experiments showed, moreover, that pulse charge is almost constant with field and temperature. Therefore, the soliton charge will be a property of the polymer material rather than the electrode-polymer interface, as observed in the charge pulses detected for the two mini-cables with different carbon-loaded electrodes. The compression takes a different form depending upon the polarity of the soliton pulse, with negative solitons associated with the concomitant shear produced by β-mode displacements and the positive solitons

TABLE V. Pulse charge for two different XLPE-based insulating materials (INS1 and INS2), E = 40 MV/m, T = 308K.

Pulse Polarity	Material	Pulse charge [C/m^2]
Positive	INS 1	2.0×10^{-5}
	INS 2	1.3×10^{-5}
Negative	INS 1	1.0×10^{-5}
	INS 2	0.8×10^{-5}

with γ-mode displacements. Both these displacements take place in the amorphous fraction of polyethylene and are non-interactive,[39] i.e., polymer chains involved in the β-mode relaxation are not involved in the γ-mode relaxation and vice versa. It is this which allows the pulses to pass one another in the same plane without neutralization, as a positive hole of the positive soliton can never come into direct contact with an electron in the negative soliton without an independent hopping transfer which takes much longer than the passage of the solitons.

The model that we have presented should apply to all compressible insulating polymers. We have demonstrated that it is not just restricted to XLPE cable insulation by a series of experiments on a cycloaliphatic epoxy resin with and without a loading of Bohemite nano-particles (3–7% by weight). These experiments were performed on 0.3 mm flat slabs in a PEA system with a carbon-loaded polyethylene as the high voltage electrode but aluminum as the earth electrode above the piezo-electric sensor. Preliminary results were presented in Fabiani *et al.*[47] and more details are given in Montanari *et al.*[48] Soliton pulses of both polarity were observed in all of the Bohemite loaded samples at E = 20MV/m and 30MV/m and temperatures of 293 – 313 K with a magnitude ($1-2 \times 10^{-6}$ Cm^{-2}) that was much smaller than those observed in the XLPE-insulated mini-cable, but with similar repetition rates. In these materials also we confirmed the correlation between the charge solitons measured via the PEA system and current pulses. The mobility of the soliton pulses in these materials was $1-2 \times 10^{-10}$ m^{2}V^{-1}s^{-1}, i.e., about 1/3 of those found in the mini-cable, but it was still many orders of magnitude larger than that expected for charge carriers in steady state currents. A summary of the data for E = 20 MV/m and T = 293 K is given in Table VI. The activation energies determined for the positive and negative solitons were in the range 0.1–0.17 eV, i.e., different to those found in XLPE, as would be expected since epoxy resins are network polymers rather than semicrystalline as is XLPE and the compression would involve the displacement of unfulfilled cross-links with lower activation energies. Evidence for soliton transport was only found in the pure epoxy resin when an external pressure was applied, which we believe increased the compression at the electrodes above the onset level for pulsive injection. These results show that the charge soliton conduction is not limited to polyethylene, or cable (cylindrical geometry), or to the presence of carbon-loaded polyethylene electrodes. It is a general feature of conduction in compressible polymers.

TABLE VI. Summary of results for charge soliton pulses in Bohemite loaded epoxy resin, E =20MV/m, T = 293K.

Pulse Polarity	Material	Mobility (m^2/Vs)	Charge/Area (Cm^{-2})	Repetition Rate (s^{-1})
Positive	Epoxy + 3%	1.38×10^{-10}	1×10^{-6}	2
	Epoxy +5%	1.1×10^{-10}	4×10^{-6}	3
	Epoxy +7%	1.4×10^{-10}	2.3×10^{-6}	3
Negative	Epoxy + 3%	1.2×10^{-10}	1.44×10^{-6}	2.5
	Epoxy +5%	—	4×10^{-6}	3.5
	Epoxy +7%	1.22×10^{-10}	2.3×10^{-6}	2

VI. CONCLUSIONS

Evidence has been presented that shows that electrical currents in compressible insulating polymers under dc electric fields are not always a continuous flow of charge. Instead the currents may include charge soliton transport of injected charge giving charge pulses containing about 10^9 electronic charges, whose mobilities are many orders of magnitude higher than that of independent carriers in steady state currents. This phenomenon takes place at electric fields in the range 10–50 MV/m, and has been shown to be consistent with a discontinuous pulsive injection process in which the injected charge relaxes electromechanical compression at the electrode. In XLPE the transport of the charge pulse has been shown to be consistent with a model in which it is represented as a soliton comprised of a coherently moving charged compression boundary.

[1]N. F. Mott and R. W. Gurney, *Electronic Processes in Ionic Crystals* (Clarendon, Oxford, 1948).
[2]J. J. O'Dwyer, *The Theory of Electrical Conduction and Breakdown in Solid Dielectrics* (Clarendon, Oxford 1973).
[3]D. A. Seanor, *Electrical Properties of Polymers* (Academic, London, 1982).
[4]L. A. Dissado and J. C. Fothergill, *Electrical Degradation and Breakdown in Polymers* (P. Peregrinus, London, 1992).
[5]A. Rose, Phys. Rev. **97**, 1538 (1955)
[6]A. Many and G. Rakavy, Phys. Rev. **126**, 1980 (1962).
[7]G. C. Montanari, IEEE Trans. Dielectr. Electr. Insul. **7**, 309 (2000).
[8]S. Hole, C. Alquie, and J. Lewiner, IEEE Trans. Dielectr. Electr. Insul. **4**, 719 (1997).
[9]N. Hozumi, T. Takeda, H. Suzuki, and T. Okamoto, IEEE Trans. Dielectr. Electr. Insul. **5**, 82 (1998).
[10]G. C. Montanari and D. Fabiani, IEEE Trans. IEEE Trans. Dielectr. Electr. Insul. **7**, 322 (2000).
[11]A. See, J. C. Fothergill, L. A. Dissado, and J. M. Alison, Meas. Sci. Technol. **12**, 1227 (2001).
[12]S. Hole and J. Lewiner, Phys. Rev. B. **64**, 104106 (2001).
[13]D. Fabiani, G. C. Montanari, L. A. Dissado, C. Laurent, and G. Teyssedre, IEEE Trans. Dielectr. Electr. Insul. **16**, 241 (2009).
[14]M. Fukuma, M. Nagao, N. Hozumi, M. Kosaki, Y. Kohno, K. Fukunaga, and T. Maeno, IEEE Conf. Electr. Insul. Dielectr. Phenom. **1**, 550 (2002).
[15]M. Zhan, C. F. Tsang, and S.-C. Pao, J. Appl. Phys. **45**, 2432 (1974).
[16]R. Liu and T. Takada, J. Phys. D. Appl. Phys. **26**, 986 (1993).
[17]T. Maeno and K. Fukunaga, IEEE Trans. Dielectr. Electr. Insul. **3**, 754 (1996).
[18]N. Hozumi, T. Takeda, H. Suzuki, and T. Okamoto, IEEE Trans. Dielectr. Electr. Insul. **5**, 82 (1998).
[19]R. Lui, T. Takada, and N. Takasu, J. Phys, D. Appl. Phys. **26**, 986 (1993).
[20]S. Hole, T. Ditchi, and J. Lewiner, Phys. Rev. B. **61**, 13528 (2000).
[21]S. Delpino, D. Fabiani, G. C. Montanari, L. A. Dissado, C. Laurent, and G. Teyssedre, IEEE Conf. Electr. Insul. Dielectr. Phenom. **1**, 421 (2007).

[22]L. Ying, M. Yasuda, and T. Takada, IEEE Trans. Dielectr. Electr. Insul. **1**, 188 (1994).
[23]D. Fabiani, G. C. Montanari, and L. Dissado, IEEE Int. Conf. Prop. Appl. Dielect. Mater. **1**, 337 (2009).
[24]H. Kon, Y. Suzuoki, T. Mizutani, M. Ieda, and N. Yoshifuji, IEEE Trans. Dielectr. Electr. Insul. **3**, 380 (1996).
[25]A. See, L. A. Dissado, and J. C. Fothergill, IEEE Trans Dielectr. Electr. Insul. **8**, 859 (2001).
[26]G. Teyssedre, C. Laurent, G. C. Montanari, F. Palmieri, A. See, L. A. Dissado, and J. C. Fothergill, J. Phys. D. **34**, 2830 (2001).
[27]G. Mazzanti, G. C. Montanari, and J. M. Alison, IEEE Trans Dielectr. Electr. Insul. **10**, 187 (2003).
[28]J. P. Jones, J. P. Llewellyn, and T. J. Lewis, IEEE Trans. Dielectr. Electr. Insul. **12**, 951 (2005).
[29]F. Boufayed, G. Teyssedre, C. Laurent, S. Le Roy, L. A. Dissado, P. Segur, and G. C. Montanari, J. Appl. Phys. **100**, 104105 (2006).
[30]K. Matsui, Y. Tanaka, T. Takada, and T. Maeno, IEEE Trans. Dielectr. Electr. Insul. **15**, 841 (2008)
[31]S. Pelissou, H. St-Onge, and M. R. Wertheimer, IEEE Trans. Electr. Insul. **23**, 325 (1988).
[32]T. J. Lewis, J. P. Llewellyn, and M. J. van der Sluijs, IEE Proc. A **140**, 385 (1993).
[33]D. M. Taylor and T. J. Lewis, J. Phys. D: Appl. Phys. **4**, 1346 (1971).
[34]J. Bylander, T. Duty, and P. Delsing, Nature **434**, 361 (2005).
[35]S. Gronenborn, B. Sturman, M. Falk, D. Haertle, and K. Buse, Phys. Rev. Lett. **101**, 116601 (2008).
[36]P. Morin, J. Lewiner, C. Alquie, and T. Ditchi, p. 43–57, in *Space Charge in Solid Dielectrics* (Dielectrics Society, Leicester (UK), 1998)
[37]S. Serra, E. Tosatti, S. Iarlori, S. Scandolo, and G. Santoro, Phys. Rev. B. **62**, 4389 (2000).
[38]J. Artbauer, J. Phys. D. Appl. Phys. **29**, 446 (1996).
[39]R. H. Boyd, Polymer **5**, 1123 (1985).
[40]J. P. Crine, IEEE Trans. Electr. Insul. **22**, 169 (1987).
[41]T. J. Lewis, IEEE Trans. Dielectr. Electr. Insul. **9**, 717 (2002).
[42]D. K. Davies, J. Phys. D: Appl. Phys. **2**,1533 (1969).
[43]T. J. Fabish and C. B. Duke, J. Appl. Phys. **48**, 4256 (1977).
[44]G. Blaise, J. Appl. Phys. **77**, 2816 (1995).
[45]F. Zhang and M. A. Collins, Phys Rev. E. **49**, 5804 (1994).
[46]A. A. Zubova and N. K. Balabaev, J. Nonlinear Math. Phys. **8**, 305 (2001).
[47]D. Fabiani, G. C. Montanari, and L. Dissado, IEEE Conf. Electr. Insul. Dielectr. Phenom. **1**, 31 (2009).
[48]G. C. Montanari, D. Fabiani, and L. A. Dissado, "A New Phenomenon in Dielectric Material Physics: Ultra-fast Soliton Conduction", J. Polym. Science B (submitted) (2011).